PAPER

AquaOptical: A Lightweight Device for High-rate Long-range Underwater Point-to-Point Communication

AUTHORS

Marek Doniec
Carrick Detweiler
Iuliu Vasilescu
MIT Computer Science and Artificial Intelligence Laboratory (CSAIL)

Mandar Chitre
Matthias Hoffmann-Kuhnt
Acoustic Research Laboratory (ARL), National University of Singapore

Daniela Rus
MIT Computer Science and Artificial Intelligence Laboratory (CSAIL)

ABSTRACT

This article describes AquaOptical, an underwater optical communication system. Three optical modems have been developed: a long-range system, a short-range system, and a hybrid system. We describe their hardware and software architectures and highlight trade-offs. We present pool and ocean experiments with each system. In clear water, AquaOptical achieved a data rate of 1.2 Mbit/s at distances up to 30 m. In water with visibility estimated at 3 m, AquaOptical achieved communication at data rates of 0.6 Mbit/s at distances up to 9 m.

Keywords: Underwater, Wireless, Optical communication

Introduction

Our goal is to develop persistent long-term ocean observatories that can monitor and survey underwater habitats. To this end, we are developing underwater sensor networks (Vasilescu et al., 2005; Vasilescu et al., 2010; Detweiler et al., 2007). An underwater sensor network integrates computation, communication, sensing, and supporting algorithms. Both hardware and software components of the system have to address the characteristics of the sub-sea environment. A critical component of an underwater observatory is its ability to transmit data collected *in situ* from sensors. Traditionally, underwater communications used acoustic communications, which achieve long-distance broadcast at slow data rates with high-power consumption. Two examples are the commercially available, the WHOI acoustic modem (Freitag et al., 2005) and the Benthos modem (Teledyne Benthos, 2010).

In this article, we investigated optical communication as an alternative to acoustic communication for communication underwater. Optical communication underwater has the potential to achieve much higher data transfer rates than an acoustic communication system at significantly lower power consumption, simpler computational complexity, and smaller packaging. However, they operate in a point-to-point communication setting, where both the receiver and the transmitter are usually directional and require alignment for the communication to work effectively. Further, their range and scope are affected by the water clarity, water light absorption, and power loss because of propagation spherical spreading. We believe that an effective method for uploading large-scale data collected by an underwater sensor network is to use data muling, where a robot equipped with an optical modem will visit each node of the sensor network and upload its data while hovering within optical communication range. In our previous work (Vasilescu et al., 2005), we have built and demonstrated an underwater sensor network system capable of optical data muling. However, the performance of the optical modems was low. This article describes a second-generation optical communication system that improves over the previous version in data rate, range, power use, and capability.

We build on underwater optical communication research by other groups. A number of studies explore the theory of optical transmission in water (Fung and Ercan, 2009; Smart, 2005; Snow et al., 1992; Cochenour et al., 2006; Laux et al., 2002). An early underwater analog communication system was reported by Tsuchida et al. (2004). It uses infrared light to transmit crayfish neuronal activity information from a live crayfish in an aquarium. There are a few recent studies exploring possible techniques and systems for underwater optical communication (Channey, 2005; Giles and Bankman, 2005; Schill et al., 2004). Farr et al. (2006) conclude that using

optical communication is the only way to achieve high data rates underwater. They discuss the possibility of using optical communication for control of underwater vehicles and present the results of an early prototype optical communication system. Using optical communication for controlling underwater robotics swarms is suggested in Fung and Ercan (2009). Recently, the use of waveguide-modulated optical lasers has been proposed for high-speed optical communication (Hanson and Radic, 2008). They report error-free underwater optical transmission measurements at 1 Gbit/s over a 2-m path in a laboratory water pipe with up to 36 dB extinction. The setup requires an optically pumped 1-W laser that is converted to the appropriate wavelength by the use of a PPLN crystal. This makes an omnidirectional transmitter very difficult. Further, the device is large and complex because of the difficulty in directly modulating a green laser at high speed. We reported the first use of optical networking underwater by Vasilescu et al. (2005) and Dunabin et al. (2006). This article builds on a previous version of this work, which was presented by Doniec et al. (2009).

AquaOptical Hardware

We have developed three optical communication systems: the long-range optical modem (called AquaOpticalLong), the short-range optical modem (called AquaOpticalShort), and a hybrid optical modem (called AquaOpticalHybrid), a cross between the other two. Our goal with this work was to study the space of design and performance for optical modems and to identify trade-offs in this space. The long-range optical modem has been designed to operate distances on the order of tens of meters and communication rates on the order of 1 Mbit/s at low power. The short-range optical modem has been designed to operate at distances on the order of 1–5 m and data rates on the order of 1 Mbit/s. There are significant hardware and software differences between these modems as described in the next sections. The main trade-offs are between cost, distance, and performance.

Long-range Optical Modem

AquaOpticalLong consists of two components, an optical transmitter and an optical receiver, each of which is contained in water-tight tubes of 8-cm diameter and 26.7- and 38.1-cm length, respectively. The transmitter weights 1500 g and the receiver 2075 g. The transmitter consists of an array of six 5-W LEDs that emit 480 nm light. They can be operated at up to 5 MHz with a minimum pulse length of 100 ns. An field-programmable gate array (FPGA) is used to encode a raw data stream into symbols for the physical layer using discrete pulse interval modulation (DPIM; see Figure 1). Each byte is converted into four symbols, each of which is represented by a different length pause between two consecutive light pulses. Figure 2 shows an overview of the long-range optical modem receiver. The receiver consists of an Avalanche Photo-diode, which includes a low-noise amplifier and is thermoelectrically cooled. An analog-to-digital converter (ADC) converts the resulting signal into a stream of 12-bit words by sampling at 40 Mega samples per second. A primary stage FPGA then filters the digitized data stream. Inside the FPGA, the signal is filtered using a matched filter (MF) and then digitized into a pulse train using a threshold filter. The digital output from

FIGURE 1

DPIM: Each bit pair is represented by a different distance between two successive light pulses.

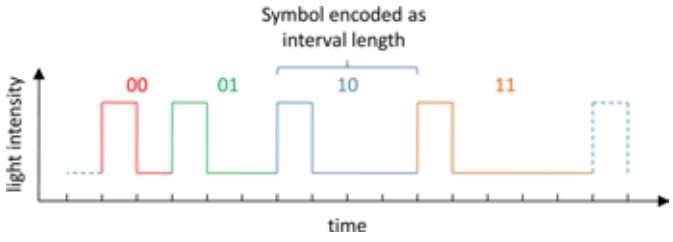

FIGURE 2

The long-range optical modem receiver using an MF. The incoming signal is first digitized at up to 40 Mega samples per second. An MF corresponding to the expected pulse shape is then applied to the signal. Finally, a threshold filter is used for pulse detection.

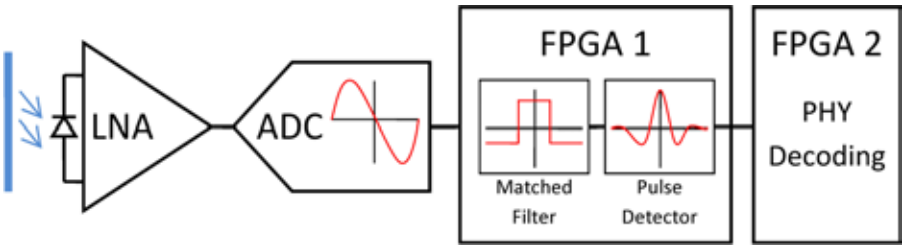

the primary stage FPGA is fed into a secondary stage FPGA, which serializes it into a byte stream. The packets are delimited by a fifth symbol whose pulse length is larger than the other symbols used to encode data. Each packet begins with a 4-byte header consisting of transmitter address, receiver address, packet length, and packet type and terminates with a cyclic redundancy check (CRC) byte. Figure 3 shows the optical modem prototype. This version of the modem does not include error correction.

FIGURE 3

The receiver and transmitter of AquaOpticalLong.

A previous version of the AquaOpticalLong receiver used a variable gain amplifier (VGA) in conjunction with an analog threshold filter to digitize the incoming signal. We replaced this setup with the ADC and the first stage FPGA. In the experimental section of this article, we refer to this previous version as the AquaOpticalLong with VGA. We refer to the new version as AquaOpticalLong with MF.

Short-range Optical Modem

The high-level architecture of the short-range optical modem is similar to the architecture of the AquaOpticalLong. It includes an optical receiver and an optical transmitter.

The short-range receiver uses a commonly available and inexpensive photodiode produced by Advanced Photonix, Inc. (part number PDB-C156). The actual sensor of the diode is 8.02 mm^2 large and has a response of 14–18 A per watt of light received. The output of the diode is digitized using an IrDA receiver chip produced by Linear Technology (part number LT1328). Just as with the long-range model, the digitized output is decoded using an FPGA and serialized into a byte stream. The packets are delimited by a fifth symbol whose pulse length is larger than the other symbols used to encode data. Each packet begins with a 4-byte header containing transmitter address, receiver address, packet length, and packet type and terminates with a CRC byte.

The short-range transmitter consists of one of the units used by the long-range optical system, which is a 5-W LED that emits 480 nm light. An FPGA is used to encode a raw data stream into symbols for the physical layer using DPIM. Each byte is converted into four symbols, each of which is represented by a different length pulse.

In contrast, the long-range receiver uses an array of six LEDs for transmission and an avalanche photodiode, which is far more sensitive than the photodiode used in the short-range system and much more expensive. The costs of an avalanche photodiode with the primary control circuitry are two orders of magnitude higher than those of a simple photodiode such as the PDB-C156. Thus, the advantages for the PDB-C156 diode and the LT1328 combination are as follows:

- small size (see Figure 4),
- easy to use/control,
- low power consumption,
- low heat dissipation,
- and low cost.

FIGURE 4

The receiver and transmitter of AquaOpticalShort can be seen on the left. A sensor node with the short-range receiver and transmitter integrated in the top cap is displayed on the right.

Its disadvantages are as follows:

- a worse signal response than the avalanche diode
- and digitization of the signal at an early stage (no low-noise amplifier, just a preamp), thus losing possible information.

The advantages for the long-range modem are as follows:

- higher sensitivity,
- better amplifiers (this making the detection of very weak pulses possible and increasing communication range)

The disadvantages are as follows:

- size (more than 10 times the volume of the PDB-C156/LT1328 assembly),
- its power consumption (5 W for cooling and additional power for control),
- the resultant heat dissipation which requires active cooling and a large heat sink, and
- its significantly higher cost.

Hybrid Optical Modem

We designed the hybrid optical modem to enhance the performance of the short-range modem by using

the more powerful transmitter of the long-range system and the lower cost receiver of the short-range system.

AquaOptical Software

The software of AquaOptical consists of two modules: the symbol encoder/decoder and the packet encoder/decoder. The symbol encoder is located inside the FPGA, the packet encoder, and the decoder run on the CPU of the sensor node, while the symbol decoder is split between the FPGA and the CPU of the sensor node.

The packet encoder takes payload data of 1–250 bytes and a destination byte as input. It constructs a valid packet by creating the 4-byte header (source, destination, type, and length) as well as computing and appending the CRC byte. It then sends the packet over a serial peripheral interface bus to the symbol encoder located inside the FPGA.

The symbol encoder receives each packet as a stream of bytes as input. Each byte is split into 4 bit pairs. The packet is processed first to the last byte. The most significant bit (MSB) of each byte are processed first, the least significant bit (LSB) last. The first light pulse sent marks the beginning of the packet. A synchronous counter running at 16 MHz times the distances between successive light pulses to encode the symbols. The duration of the light pulses generated as well as of the different pauses used for the four possible symbols can be configured in software.

The symbol decoder front end is running inside the FPGA. It takes as input the digitized output of the photodiode. When the first pulse is received, a new decoding cycle starts. A 16-MHz counter times the distance between successive pulses. After each pulse, the new distance is stored inside a FIFO. If the distance counter exceeds the maximum count (255), the value 255 is written into the FIFO and the counter simply waits for the next pulse to start.

The actual decoding of the symbols takes place inside the CPU. The CPU polls the bytes from the FPGA using the serial peripheral interface bus. Each distance is converted into a bit pair using software configurable threshold values. Every four successive bit pairs are packed into a byte, which is written into a buffer. When a distance larger than a packet timeout threshold is read, the packet decoder is called to process the current buffer contents.

The packet decoder checks if the CRC of the buffer is 0 and if the packet is addressed to this sensor node. It then calls the handler for the data.

The FPGA contains the symbol layer encoder and front end of the decoder in order that both can run asynchronously to the CPU. In addition, this ensures that packet encoding and decoding are not influenced by other processes running on the same CPU.

Power Consumption

All three versions of AquaOptical share the same sensor node design and thus the same energy source design. Each device contains six lithium polymer cells with a capacity of 9.62 Wh (3.7 V, 2.6 Ah). The cells are arranged in a 3 × 2 configuration yielding an average voltage of 11.1 V and a capacity of 5.2 Ah or 57.72 Wh. This energy has to be shared between the sensor board and the communication hardware of the optical modem (LEDs, drivers, APD, amplifiers, and decoder).

The sensor board consumes an average of 100 mW when running in active mode without radio and GPS enabled. It can sleep when not receiving data, at which point it consumes about 1 mW.

Power Consumption for the Transmitter

The AquaOpticalShort transmitter design drives a single LED at 5 W strong pulses. The current limiting resistor drops an additional 1.4 W, resulting in a total pulse power of 6.4 W. The current encoding architecture pulses the LEDs at an average duty cycle of 1/3, resulting in an average power consumption of 2.1 W. Together with the sensor board, this results in a total power consumption of 2.2 W and a theoretical run time of over 26 h.

The AquaOpticalLong transmitter uses six of the same LEDs resulting in a total power consumption of 12.9 W and a theoretical run time of 4 h 28 min.

There are multiple ways to extend this run time. Some of these only require software changes and some extensions to the hardware.

The easiest method is to drop the duty cycle significantly. We currently run the modem with a 1/3 duty cycle at 600 Kbps, resulting in an average pulse length of 1 µs. This length was chosen to enable easier measurement of pulses and to distinguish them from ambient noise. Changing pulse width can be done in software and requires a change in the FPGA programs for both encoder and decoder. The theoretical limit is the minimum time it takes for the LEDs to switch fully on, which we measured to be around 100 ns. Since every pulse carries two bits of information, we can express a simple relationship between data rate and power consumption. For AquaOpticalLong, this relationship for the current encoding scheme (DPIM) is 3.84 W/Mbps, given a pulse length of 100 ns. The maximal theoretical

data rate resulting from 100-ns pulse width and DPIM is 3.3 Mbps, resulting in a power consumption of 12.8 W. However, if we run the modem at 600 Kbps with 100-ns pulses, our power consumption drops to 2.4 W total, resulting in a theoretical run time of 24 h.

Power Consumption for the Receiver

The AquaOpticalShort receiver consumes below 20 mW, which is less than the sensor node itself. This design can theoretically operate for over 20 days.

The AquaOpticalLong receiver consumes power for three different tasks. The first is the cooling of the APD, which, according to specifications, consumes between 4 and 9.5 W depending on the cooling needed. The second is the drive circuitry for the APD together with the LNA, which, according to specifications, consumes between 1.8 and 3.2 W. Finally, the decode stage (MF, pulse detection) consumes 100 mW to drive the ADC and the FPGA, which runs the MF and the pulse detector. We measured the power consumption of the entire receiver system to be 6 W in complete darkness, 7.2 W at ambient office light levels, and 15 W when saturated by a halogen light.

When the receiver is actually operating, its power consumption lies in the range between the ambient light measurement and the saturated sensor measurement. Thus, we predict runtime to be 4 h in the worst case scenario.

As with the transmitter, there are multiple ways to improve runtime for the receiver. First, a better optical filter can be used that lets a narrower bandwidth of light pass. This has to be well tuned with the transmitting LEDs. The current filter was chosen to well cover the entire emission spectrum of the chosen LEDs and is 20 nm wide. However, if the light source were to be confined to a smaller band gap like 10 nm, then a 10-nm filter would halve the amount of ambient light polluting the sensor. This would directly result in a significant cooling costs reduction. Assuming that the APD heats up linearly with incident light, then cooling power consumption could be cut by up to half.

Another way to reduce energy is to use a form of time domain multiple accesses in which the APD is switched on for certain time windows during which a request for data transfer has to be sent. This could reduce heat buildup in the APD and would again cut cooling power consumption. As an example, the request windows could be 10 ms long in each 100-ms interval, resulting in a 10% duty cycle when no transfers are requested. The disadvantage of this method is, however, the increased latency and the need for synchronized clocks between transmitter and receiver.

Experiments

We implemented and packaged the AquaOptical systems. We conducted several experiments in the air, in the pool, and in the ocean in Singapore Harbor.

Air Transmission Experiment

The air transmission experiments were done in an urban environment on the MIT campus. This experiment was conducted after dark to avoid sensor saturation through direct sunlight exposure. Significant ambient noise was present from street lamps and light from buildings. We only tested the AquaOpticalLong using an MF. Two scientists held and aimed the transmitter and receiver at each other. The optical modem recorded data transmission with 100% success rates at a data rate of 1.2 Mbit/s and distances up to 160 m. The transmission success rate decreased to 70% at 200 m, which was the maximum measured distance.

Pool Experiments

The pool experiments were performed in clear water. The optical modem recorded data transmission with 100% success rates at data rates up to 1.2 Mbit/s for all the distances tested. In this set of experiments, the maximum distance tested was 30 m because of the dimensions of the pool in which we conducted the experiments. We expect good optical communication performance in clear waters at distances up to 50 m.

Field Experiments in the Ocean 1

Four sets of field experiments were conducted in the ocean at a location between outlying islands south of Singapore. The big challenge for these experiments was achieving optical communication in low visibility environments. At the experimental site, human divers estimated the water visibility to be 3 m for the first three sets and 1.5 m for the last experiment. The goals of these experiments were as follows:

1. To measure the success rate of the long-range optical modem system with a VGA at various distances up to 10 m.
2. To measure the success rate of the short-range optical modem system at various distances up to 3 m using blue and green light for comparison.

3. To measure the success rate of the hybrid optical modem system consisting of the long-range sender and the short-range receiver. Because the short-range modem system is much less expensive than the long-range system, such a hybrid configuration might be used for data muling with a robot carrying the long-range receiver and a sensor network with multiple nodes equipped with the short-range receiver.
4. To measure the success rate of the long-range optical modem system with an MF receiver at various distances up to 10 m.

Experimental Setup

We conducted a suite of experiments to evaluate the performance of the three optical modem systems described in this article in the ocean. The first three experiments were conducted near a barge south of the Singapore Harbor. The water visibility during these experiments was estimated by human divers at 3 m. Figure 5 shows the basic experimental setup for the field evaluations of the optical modems. For the short-range experiments, we suspended a rigid 4-m-long rod below the boat at a depth of 4 m measured from the top of the water. Before submersing the rod, we measured and marked distances on the rod in 50-cm increments. Two divers were used in each experiment. One diver carried the transmitter unit and the other carried the receiver unit. The divers were connected to the researchers on the boat using an audio communication system integrated in the diving mask. The receiver was connected to a computer on the boat to provide visual feedback about the experiment and to debug information. The diver holding the receiver was instructed to hold the

FIGURE 5

Top: experimental setup for the long-range VGA optical modem evaluation. Middle: experimental setup for the short-range optical modem evaluation. Bottom: experimental setup for the long-range MF optical Modem evaluation.

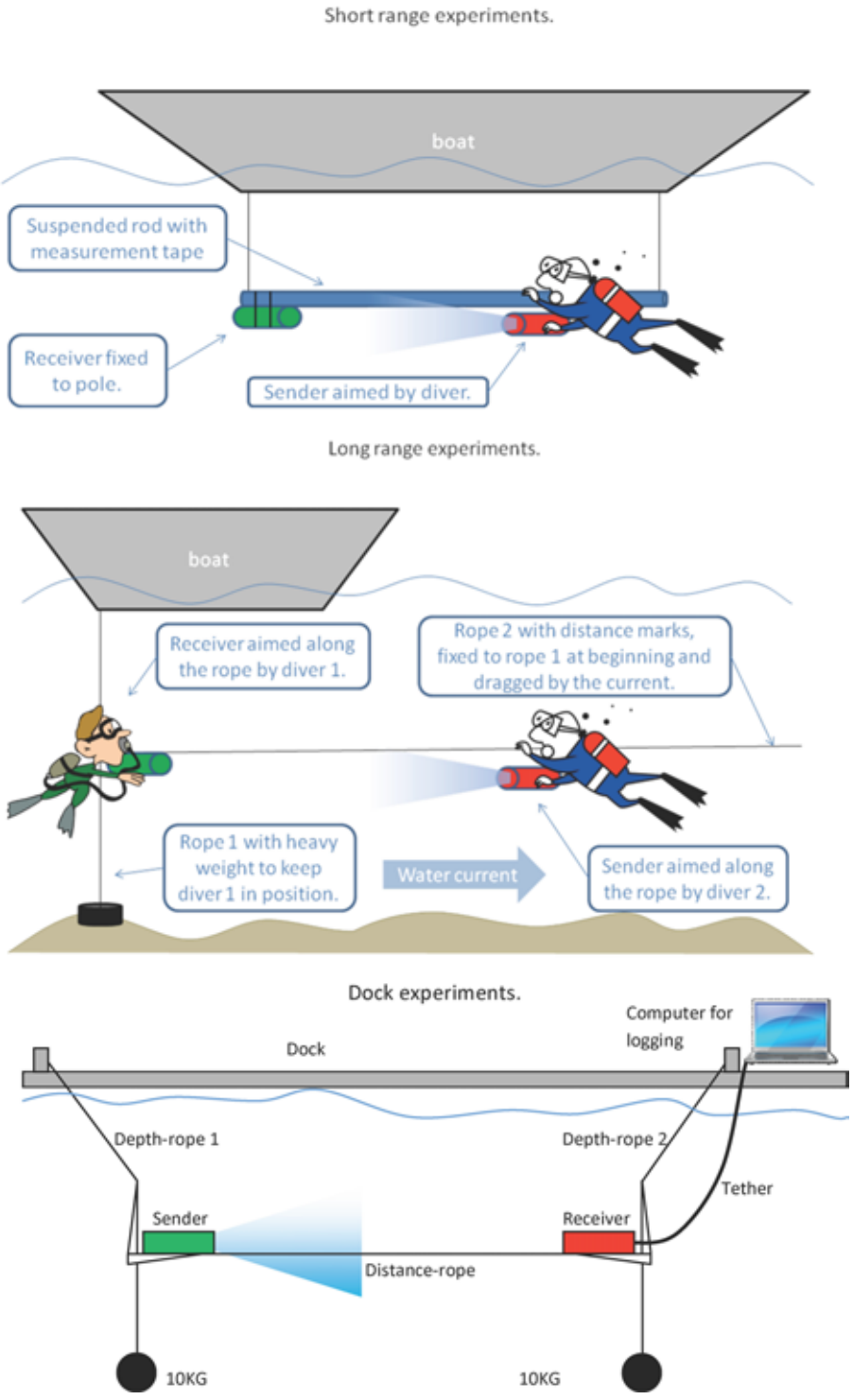

receiver parallel to the rod at position 0. This diver maintained this location for the duration of the experiment. The diver holding the transmitter was given a series of voice instructions. He was first instructed to go to the position marked 1 m (which was measured to be 1 m away from the fixed receiver) and hold the transmitter parallel to the rod, aimed at the receiver. He maintained this position for 1 min, and data were collected for 30 s at a data rate of 0.6 Mbit/s. The diver was then instructed to move further back in 50-cm increments, each time maintaining the transmitter position at the current location for approximately 1 min.

A similar experiment was conducted for the long-range optical modem. Since our expectation in this case was communication at a much further distance than in the short-range evaluations, we used a rope instead of a rod. The use of a rope allowed us to point the receiver and transmitters at each other at distances greater than what the human eye could see. We attached the rope used to measure the distance between the long-range optical modem transmitter and the receiver to a vertical rope that was fixed to the boat and kept taut by weights. The first diver with the receiver was stationed at the attachment point of the measuring rope to the vertical rope. He pointed the receiver along the measuring rope. The second diver who was holding the transmitter moved along the measuring rope and pointed the transmitter along the rope in the direction of the receiver. The measuring rope was kept taut by the water currents present.

The fourth and final experiment was conducted off the dock at the Republic of Singapore Yacht Club. The water visibility was estimated to be 1.5 m by lowering the optical modem on a rope until it was no longer visible. The experimental setup can be seen in Figure 5. The transmitter and the receiver were mounted to metal L-shaped brackets that were connected with a rope to set a distance between the modems. Each bracket was further held by a depth rope that allowed us to adjust both the depth and the tension on the distance rope. A 10-kg weight was attached with a rope to each bracket. By moving the fixture points of the depth ropes on the dock, we were able to adjust the angle at which the transmitter and the receiver were aimed. Depth could also be adjusted with the depth ropes. The disadvantage of this setup was that once the modems were out of sight (because of water turbidity), we could only estimate the angle at which they were aimed.

Short-range Optical Modem Evaluation Data

Specifically, for the short-range experiments, a single 5-W LED was used in the transmitter. Two experiments were conducted: one with a blue LED (470 nm) in the transmitter and one with a green LED (530 nm). The radiant flux generated by the LEDs is roughly equivalent to 10% of the power input, or 500 mW. The receiver uses an off-the-shelf photodiode. The short-range experiments were conducted with a throughput of 1.2 Mbit/s or 1.75 µS/symbol average.

All experiments were conducted at 4 m water depth. For the short-range experiments, a 4-m-long pole was suspended off the boat to float horizontally at 4 m depth in alignment with the water current. The short-range receiver was mounted at one end of the pole and pointed along the pole. It was tethered through a cable to allow for supervision and data logging. A measuring tape was attached to the pole. A diver was holding the transmitter and positioning it at the appropriate distances along the pole. The diver tried at all times to point the modem along the pole. At each recorded distance, the diver stayed for at least 20 s and continuously pointed the transmitter along the pole toward the receiver. Measurements were taken and binned in 2-s intervals. Each measurement consisted of the number of valid packets received and a histogram of pulse lengths received in that 2-s interval.

Figure 6 shows the experimental data with the short-range optical modem using green (green lines) and blue (blue lines with circles) light. We expected to see blue light outperform the green light as predicted by the literature. However, we observed green light to be more effective in Singapore waters. We believe this is due to the water color in the Singapore Harbor and surrounding areas.

The dashed lines correspond to the percentage of valid pulses received (corresponding to a symbol) divided by the total number of pulses received. Bad pulses are due to ambient noise. The solid lines show the number of valid packets received divided by the total number of packets received. Packets were 128 bytes long. Valid packets are those addressed correctly with matching CRCs.

Long-range Optical Modem Evaluation Data

For the long-range experiments, six 5-W blue (470 nm) LEDs were used in the transmitter, and an avalanche photodiode with a VGA was used in the receiver. The radiant flux on the transmitter was 3 W. The first set of long-range experiments was conducted with

FIGURE 6

Singapore optical modem experiment: short-range symbol and packet success rate using blue and green light. The *x* axis corresponds to distance. The *y* axis shows the percentage of valid pulses received (dotted line) and valid packets received (solid line). The blue lines (with circles) show results from trials using blue light. The green lines show results from trials with green light. Artifacts caused by the decoding of noise that when no signal is present have been removed in this plot for clarity.

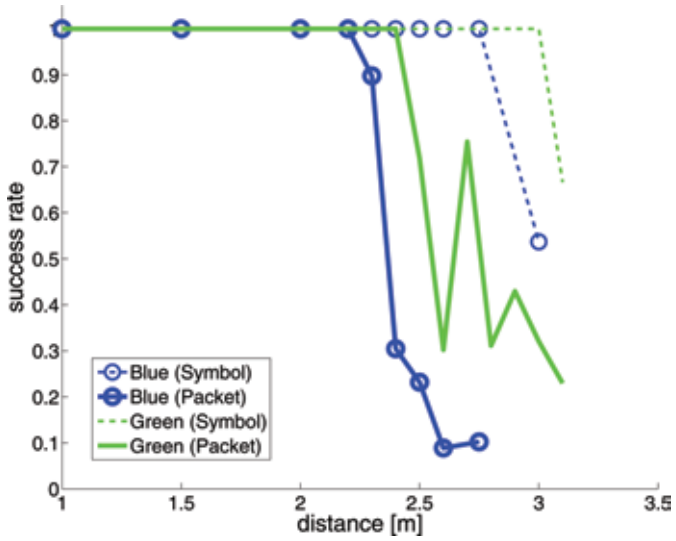

a throughput of 666 Kbits or 3 µS/symbol average. The second set of long-range experiments was conducted with a throughput of 333 Kbits or 6 µS/symbol average.

The long-range experiments were conducted in a similar fashion as the short-range experiments. However, we replaced the 4-m pole with a 12-m rope with 1-m markings that was tied to the receiver. The other end of the rope was not tethered and was floating in the current (up to 2 m/s). A diver held the receiver and tried to point it along the rope at all time. A second diver held the transmitter and was holding on to the rope while trying to point the transmitter along the rope. The rope was straight at all times because of the strong current pulling the second diver and thus straightening the rope. It was the second diver's responsibility to keep a depth of 4 m. Measurements were conducted in the same fashion as with the short-range receiver. Figure 7 shows the experimental data with the long-range optical modem taken on two different days (using blue light).

FIGURE 7

Singapore optical modem experiment: long-range (VGA) symbol and packet success rate using blue light. The *x* axis corresponds to distance. The *y* axis shows the percentage of valid pulses received (dotted lines) and valid packets received (solid lines). The black lines show results of the first day and the red lines (with circles) to the results of the second day.

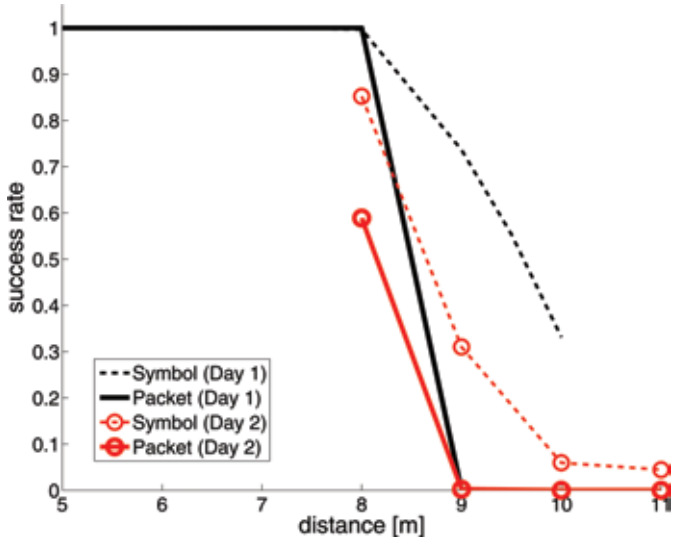

Similar to Figure 6, the dashed lines in Figure 7 correspond to the percentage of valid pulses received divided by the total number of pulses received, and the solid lines show the number of valid packets received divided by the total number of packets received. For the long-range receiver, bad pulses are due to both ambient noise and noise inside the receiving circuit due to the VGA.

An additional set of ocean experiments was conducted for the AquaOpticalLong with an MF decoder. The AquaOpticalLong with MF was tested in harbor water with a visibility of about 1.5 m, where it achieved a transmission distance of up to 8 m (five times visibility) at a data rate of 600 Kbps. In comparison, the transmission maximum distance for the experiments conducted with the VGA version of the long-range modem was 9 m, but water visibility was only 3 m. Therefore, the MF version of the long-range modem achieved five times visibility and the VGA version three times visibility. The results can be seen in Figure 8. The experiments demonstrated

FIGURE 8

Singapore optical modem experiment: long-range (MF) symbol and packet success rate using blue light. The *x* axis corresponds to distance. The *y* axis shows the percentage of valid pulses received (blue dashed line) and valid packets received (red line).

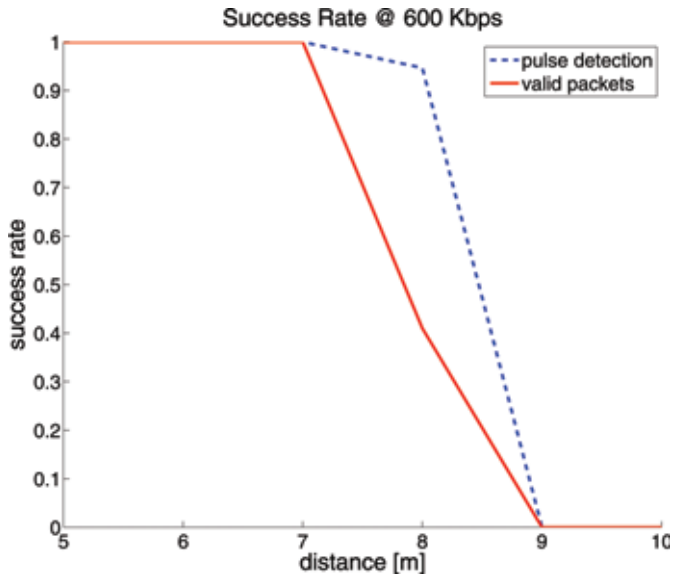

that the MF design not only improved signal detection but also almost entirely removed false positive detection of signal pulses. This can also be seen in Figure 8, where the success rate remains 0 after the maximum transmission distance. The previous design showed reception artifacts because of a high false positive rate of the VGA design.

FIGURE 9

Singapore optical modem experiment: hybrid modem success rates using the long-range optical modem sender and the short-range optical modem receiver using blue light. The *x* axis corresponds to distance. The *y* axis shows the percentage of valid pulses received (blue dashed line) and valid packets received (red line).

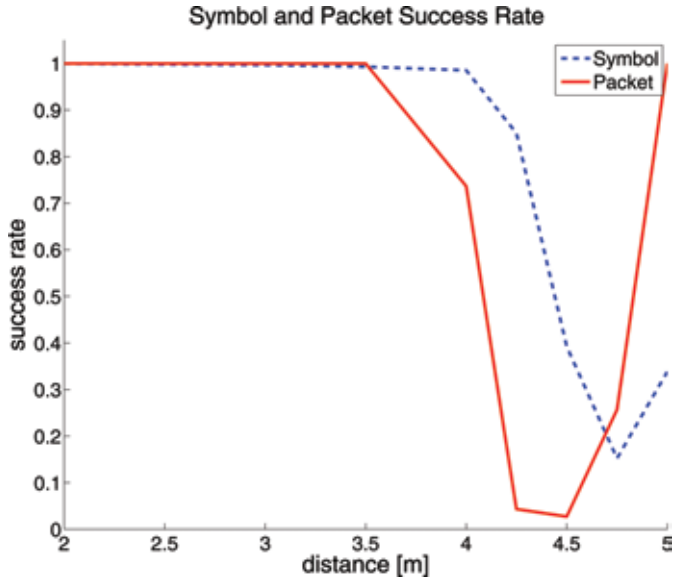

Hybrid Modem Evaluation Data

During the long- to short-range experiments, we used a short-range receiver (off-the-shelf photodiode) with our long-range 3-W radiant flux transmitter. The same procedure as in the long-range experiment was used in this case.

Figure 9 shows experiments carried out during the second day using the long-range optical modem transmitter and the short-range optical modem receiver. The blue dashed line corresponds to the percentage of valid pulses received divided by the total number of pulses received. Bad pulses are again due to both ambient noise and noise inside the receiving circuit due to the VGA. The red line is the number of valid packets received divided by the total number of packets received, where packets were again 128 bytes long and valid packets are those addressed correctly and with matching CRCs.

Discussion

Figure 10 shows the time history of one experiment. We can see how the diver conducting the experiment moved first away and then closer to the sender during the experiment. You can also see a very clear peak where the packets start arriving. The portion of the graph before the peak is noise occurring while the diver moved into position. This noise is the result of the VGA adjusting to noise levels when no valid signal is present. This problem no longer occurs in the MF design of the long-range optical receiver.

For each distance interval, the packet and the symbol success rate were measured for 30 s. The testing rate for the data transfer was 600 Kbit. Under these harsh visibility conditions, the

FIGURE 10

The timeline of a hybrid optical modem experiment. The *x* axis corresponds to discrete 2-s-long measurements. From left to right, we see the history of the experiment. The *y* axis is the packet success rate (in red) and distance (in black).

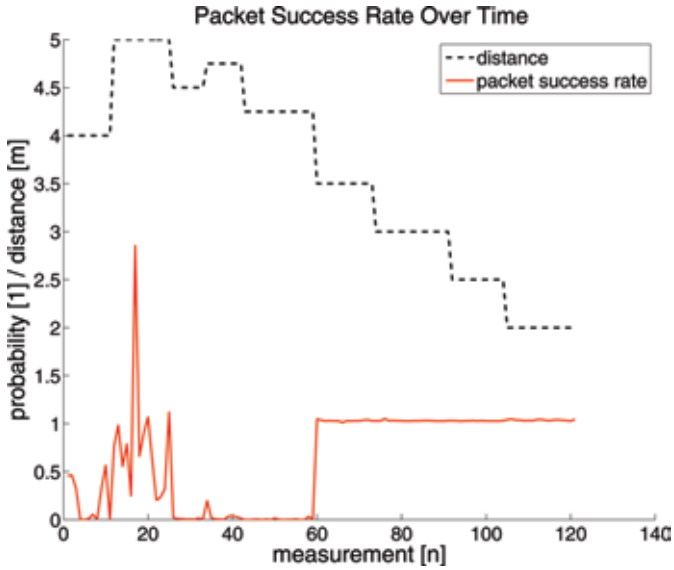

long-range optical modem achieved very close to perfect transmission rates up to 8 m. The performance degrades but is still operational up to 9.5 m. At 10 m, the receiver does not pick up any symbols.

These experiments demonstrate that the optical communication system is very well suited for data transfer at large distances (e.g., 25 m) in clear waters. The data transfer rate was good at twice the visibility range in turbid waters. We believe AquaOptical is an encouraging first step toward creating an effective optical communication system for use in data muling and other underwater data transfer scenarios. Next steps include hardware redesign for power optimization and the development of a software layer capable of both error correction and higher-level interfacing to the system.

Conclusion

This article discussed the design of a family of three underwater optical modem systems. We have designed and built three systems: a long-range optical modem, a short-range optical modem, and a hybrid optical modem. We analyzed the trade-offs between these systems and characterized their performance in the pool and in the ocean. Our preliminary experimental results suggest several hardware and software improvements to the system as well as additional experimental characterization. Our current efforts are focused on the software side to include error correction in the symbol processing and on the experimental side to evaluate the sensitivity of the systems to orientation. Next we plan to use the optical modem systems for data transfer between sensor networks equipped with the short-range modem transmitter and receiver and a robot equipped with the long-range modem transmitter and receiver.

Acknowledgments

This work was supported by the DSTA, Singapore, and the MURI Antidote project. The authors are grateful for this support. They are also grateful to the team at ARL, National University of Singapore, for providing logistical and technical support for our experiments.

Lead Author:

Marek Doniec
MIT Computer Science and Artificial Intelligence Lab
Email: doniec.@csail.mit.edu

References

Channey, M.A. 2005. Short range underwater optical communication links. Master's thesis, North Carolina State University. 117 pp.

Cochenour, B., Mullen, L., Laux, A., Curran, T. 2006. Effects of multiple scattering on the implementation of an underwater communications link. In: Proceedings of the MTS/IEEE OCEANS. pp. 1-6. Boston, MA.

Detweiler, C., Vasilescu, I., Rus, D. 2007. An underwater sensor network with dual communications, sensing, and mobility. In: Proceedings of the OCEANS—Europe. pp. 1-6. Aberdeen, Scotland.

Doniec, M.W., Vasilescu, I., Detweiler, C., Rus, D., Chitre, M., Hoffmann-Kuhnt, M. 2009. AquaOptical: a lightweight device for high-rate long-range underwater point-to-point communication. In: Proceedings of the MTS/IEEE OCEANS. Biloxi, MS.

Dunbabin, M, Corke, P., Vasilescu, I., Rus, D. 2006. Data muling over underwater wireless sensor networks using an autonomous underwater vehicle. In: Proceedings of the IEEE International Conference on Robotics and Automation, ICRA. pp. 2091-2098. Orlando, FL.

Farr, N., Chave, A., Freitag, L., Preisig, J., White, S., Yoerger, D., Sonnichsen, F. 2006. Optical modem technology for seafloor

observatories. In: Proceedings of the MTS/IEEE OCEANS. pp. 1-6. Boston, MA.

Freitag, L., Grund, M., Singh, S., Partan, J., Koski, P., Ball, K. 2005. The WHOI micro-modem: an acoustic communications and navigation system for multiple platforms. In: Proceedings of the MTS/IEEE OCEANS. pp. 1086-1092. Washington, DC.

Fung, Y.F., Ercan, M.F. 2009. Underwater short range free space optical communication for a robotic swarm. In: Proceedings of the International Conference on Autonomous Robots and Agents, ICARA. pp. 529-532. Wellington, New Zealand.

Giles, J.W., Bankman, I.N. 2005. Underwater optical communications systems. Part 2: basic design considerations. In: Proceedings of the IEEE Military Communications Conference, MILCOM. pp. 3:1700-1705. Atlantic City, NJ.

Hanson, F., Radic, S. 2008. High bandwidth underwater optical communication. Appl Opt. 47(2):277-283, doi:10.1364/AO.47.000277.

Laux, A., Billmers, R., Mullen, L., Concannon, B., Davis, J., Prentice, J., Contarino, V. 2002. The A, B, Cs of oceanographic lidar predictions: a significant step toward closing the loop between theory and experiment. J Mod Opt. 49(3/4):439-451, doi:10.1080/09500340110088498.

Schill, F., Zimmer, U.R., Trumpf, J. 2004. Visible spectrum optical communication and distance sensing for underwater applications. In: Proceedings of the Australasian Conference on Robotics and Automation, ACRA. Canberra, Austrialia.

Smart, J.H. 2005. Underwater optical communication systems. Part 1: variability of water optical parameters. In: Proceedings of the IEEE Military Communications Conference, MILCOM. pp. 1140-1146. Atlantic City, NJ.

Snow, J.P., Flatley, J.P., Freeman, D.E., Landry, M.A., Lindstrom, C.E., Longacre, J.R., Schwartz, J.A. 1992. Appl Opt. 47(2):277-283.

Teledyne Benthos. 2010. Undersea, Geophysical Equipment, Survey Sonar and ROV. http://www.benthos.com.

Tsuchida, Y., Hama, N., Takahata, M. 2004. An optical telemetry system for underwater recording of electromyogram and neuronal activity from non-tethered crayfish. J Neurosci Methods. 137:103-109, doi:10.1016/j.jneumeth.2004.02.013.

Vasilescu, I., Detweiler, C., Doniec, M.W., Gurdan, D., Sosnowski, S., Stumpf, J., Rus, D. 2010. AMOUR V: a hovering energy efficient underwater robot capable of dynamic payloads. Int. J. Rob Res. 29(5):547-570, doi:10.1177/0278364909358275.

Vasilescu, I., Kotay, K., Rus, D., Dunbabin, M., Corke, P. 2005. Data collection, storage, and retrieval with an underwater sensor network. In: Proceedings of the 3rd International Conference on Embedded Networked Sensor Systems, ACM SenSys. pp. 154-165. New York.